



Multifractals and El Naschie E -infinity Cantorian space–time

G. Iovane ^{a,*}, M. Chinnici ^b, F.S. Tortoriello ^c

^a *DIIMA, University of Salerno, Via Ponte don Melillo, 84084 Fisciano (SA), Italy*

^b *DMA, University of Naples “Federico II”, Via Cintia, Monte S. Angelo, 80126 Napoli, Italy*

^c *DIFARMA, University of Salerno, Via Ponte don Melillo, 84084 Fisciano (SA), Italy*

Accepted 16 July 2007

Abstract

The aim of this work is the analysis of multifractals in the context of Mohamed El Naschie’s $\epsilon^{(\infty)}$ Cantorian space–time applied to cosmology. As starting point we consider the results of the first author of the present paper describing scaling rules in nature, $R(N) = (h/m_n c)N^\phi$. Then, we use multifractal analysis to show that the result, already developed by the authors as Brownian motion, is a Multifractal process. Indeed, Brownian paths play a crucial role if considered to be a multifractal. Moreover, we summarize some recent results concerning fractal structure and the Brownian paths in order to calculate fractal dimension and characteristic parameters for large scale structures and for the atomic elements that live in an El Naschie’s $\epsilon^{(\infty)}$ Cantorian space–time.

© 2007 Elsevier Ltd. All rights reserved.

1. Introduction

Multifractal analysis has recently emerged as an important concept in various fields, including strange attractors of dynamical systems, stock market modeling, image processing, medical data, geophysics, probability theory and statistical mechanics, etc. [1].

Multifractal analysis is concerned with describing the local singular behaviour of measures or functions in a geometrical and statistical fashion. It was first introduced in the context of turbulence, and then studied as a mathematical tool in increasing general settings [2]. Multifractal theory has been discussed by numerous authors and it is developing rapidly [3]. Mandelbrot firstly mentioned multifractal theory in 1972. In 1986, Halsey drew attention to the concept of multifractal spectrum; that is an interesting geometric characteristic for discrete and continuous models of statistical physics. Olsen was motivated by the heuristic ideas of Halsey. In 1995, Olsen established a multifractal formalism. This formalism has been designed in order to account for the statistical scaling properties of singular measures when it happens that a finite mass can be spread over a region of phase space in such a way that its distribution varies widely. The multifractal formalism is build on the definition of the singularity spectrum which is connected to the subset of the support of the measure where singularity has a given strength namely its *Hausdorff dimension*.

* Corresponding author.

E-mail addresses: iovane@diima.unisa.it (G. Iovane), marta.chinnici@dma.unina.it (M. Chinnici), savtor@libero.it (F.S. Tortoriello).

The purpose of this work is firstly to reconsider the case of the Brownian paths in the context of El Naschie's $\epsilon^{(\infty)}$ Cantorian space–time, from the point of view of the previous model of the authors [4] and by using multifractal analysis.

As shown in [5,6] Nature shows us structures with scaling rules, where clustering properties from cosmological to nuclear objects reveals a form of hierarchy. In [7,8], the consequences of a stochastic, self-similar, fractal model of Universe was compared with observations. Indeed, it was demonstrated that the observed segregated Universe is the result of a fundamental self-similar law, which generalizes the Compton wavelength relation, $R(N) = (h/Mc)N^{1+\phi}$, where R is the radius (characteristic length) of the structures, h is the Plank constant, M is the total mass of the self-gravitating system, c the speed of light, N the number of the nucleons within the structures and $\phi = \frac{\sqrt{5}-1}{2}$ is the Golden Mean. As noted by Mohamed El Naschie, this expression agrees with the Golden Mean and with the gross law of Fibonacci and Lucas [9–11].

Starting from an universal scaling law, the author showed its agreement with the well known Random Walk equation that was used by Eddington for the first time [12,13]. In [8,14,16,17], the relevant consequences of a stochastic self-similar and fractal Universe were presented.

The main aim of this paper is to investigate the link between our previous result $\tilde{B}_N = B_N + \phi^3 N$ (indeed we will use the Brownian paths) and its multifractal nature in the context of El Naschie's $\epsilon^{(\infty)}$ Cantorian space–time [11].

Secondly, we are interested to evaluate, through the results in [17], the fractal dimension and characteristic parameters of the time for some objects.

The paper is organized as follows: Section 2 presents a short review of definitions and properties of multifractals processes and Brownian paths; Section 3 presents an astrophysical scenario; Section 4 is devoted to study the application of Brownian multifractals in the context of El Naschie's $\epsilon^{(\infty)}$ Cantorian space–time; in Section 5 we calculate the fractal dimension and the age of Universe, solar system objects and atomic elements. Finally, conclusions are drawn in Section 6.

2. Some fractal properties of Brownian paths

Models using *fractional Brownian motion* (fBm) have helped to advance the field through their ability to assess the impact of fractal features such as statistical self-similarity and long-range dependence (LRD) to performance [18]. Roughly speaking, a fractal entity is characterized by inherent, ubiquitous occurrence of irregularities which governs its shape and complexity.

First, we consider the fBm $B_H(t)$; its paths are almost surely continuous but not where $H \in (0, 1)$ is the self-similarity parameter:

$$B_H(at) = a^H B_H(t). \quad (1)$$

However, the scaling law (1) implies also that the oscillations of fBm at fine scales are uniform and this comes as a disadvantage in various situations. Indeed, fBm is a model with poor multifractal structure and does not contribute to a larger pool of stochastic processes with multifractal characteristics. Hence, in order to describe real world signals that often possess an erratically changing oscillatory behaviour (*multifractals*) fBm is not an appropriate model.

The first “natural” multifractal stochastic process to be identified is *Lévy motion* [22,23].

A Lévy process $\{(X_t), t \geq 0\}$ valued in \mathfrak{R}^d is a stochastic process with stationary independent increments. Brownian motion and Poisson processes are examples of Lévy processes that can be qualified as *monofractal*; for instance the Holder exponent of the Brownian motion is everywhere 1/2 (the variations of its regularity are only of a logarithmic order of magnitude). Most Lévy processes are multifractal under the condition that their Lévy measure is neither too small nor too large near zero. Furthermore, their spectrum of singularities depends precisely on the growth of the Lévy measure near the origin.

Before applying the multifractal analysis to our cosmological scenario, we need recall some basic definitions and results about Brownian path [24].

Let $B_d = \{B_d(t)\}$ be a *standard d-dimensional Brownian motion*; this process (also named Wiener process) is (stochastically) self-similar with index 1/2 by which it means that, for any $c \geq 0$, the time-scaled process $\{B_d(ct)\}$ and the space-scaled process $\{\sqrt{c}B_d(t)\}$ are equivalent in the sense of finite-dimensional equivalence. This self-similar property is central in our study, from which various dimension formulae concerning Brownian paths can be figured out.

Brownian sample paths exhibit highly erratic patterns, despite the continuity. Thus, this should be rich source of fractal analysis/geometry and be one prevailing topic in nonlinearity.

As well known fractal sets connected with Brownian motion can be written as

$$\begin{aligned} [B_d] &= \{x : x = B_d(t), \text{ some } t\}, \\ Z &= \{t : B_1(t) = 0\}, \\ I_d &= [B_d] \cap [B'_d], \end{aligned}$$

where B'_d denotes an independent copy of B_d . Thus, the three sets are simply the trail (range), the zero set, and the set of intersections of Brownian paths. Note that the zero set is meaningful only for the one-dimensional case, while the trail and the intersection are meaningful only for the multidimensional case. These are due to the fact that the one-dimensional Brownian motion is point-recurrent while it is not so for the multi-dim case. These sets are random, since they depend on a particular sample path realization $B_d(t, \omega)$, and so we must interpret any statement about these sets and their associated measures (random too) as being true “with probability one”.

Let $\dim K$ denote the Hausdorff dimension of a Borel K . The following results are well known:

$$\begin{aligned} d = 1 \quad \dim Z &= 1/2, \\ d \geq 2 \quad \dim [B_d] &= 2, \\ d = 2, 3 \quad \dim I_d &= d - 2(d - 2). \end{aligned}$$

There are natural measures associated with the above fractals Z , $[B_d]$ and I_d ; there are respectively Brownian *local time measure*, *occupation measure* and *intersection measure*. These measure are regarded as *fractal measures*, since each of them is singularly continuous (non-atomic and supported by a set of Lebesgue measure zero) and exhibits a certain self-similarity which is inherited from the self-similarity of the process. The main difference (and difficulty) from pure analysis is that the self-similarity is now always in the distributional sense rather than the strict (analytic) sense.

2.1. Intersection of exponents

In the present section, we give a recent results on the intersection exponents and the multifractal spectrum for measures on Brownian paths (for more details see [25]). Intersections of Brownian motion or random walk paths were studied for quite a long time in probability theory and statistical mechanics. There is trivial behaviour in all dimensions exceeding a critical exponent which determines the universality class of the model and enter into most of its quantitative studies. Finding the intersection exponents of planar Brownian motion was one of the first problems solved by the rigorous techniques based on the stochastic Loewner evolution devised by Lawler et al. (for more details see [26–28]).

Above, we have seen that an interesting geometric characteristic for discrete and continuous models of statistical physics is the *multifractal spectrum*. This evaluates the degree of variation in the intensity of a spatial distribution. A multifractal formalism is used for computing multifractal spectrum, based on a large-deviation heuristic (see [29]).

Let us give the definition of multifractal spectrum; suppose that μ is a (fractal) measure on \mathfrak{R}^d . The value $f(a)$ of the multifractal spectrum is the Hausdorff dimension of the set of points $x \in \mathfrak{R}^d$ with $d \geq 2$

$$\lim_{r \downarrow 0} \frac{\log \mu(B(x, r))}{\log r} = a, \tag{2}$$

where $B(x, r)$ denotes the open ball of radius r centered in x . In many cases of interest, the limit in (2) has to be replaced by \liminf or \limsup to obtain an interesting nontrivial spectrum. In details, in fractal geometry the relation between Hausdorff dimension and the critical exponents of statistical physics is shown with *intersection exponents*. To define the intersection exponents for Brownian motion with $d = 2, 3$, suppose $n, m \geq 1$ are integers and let W_1, \dots, W_{m+n} be a family of independent Brownian motion in \mathfrak{R}^d started uniformly on $\partial B(0, 1)$ and running up to the first exit time $T^i(r)$ from a large ball $B(0, r)$.¹ We divide the motions into two packets and look at the union of the paths in each family

$$\mathfrak{B}_1(r) = \bigcup_{i=1}^m W_i([0, T^i(r)]), \quad \mathfrak{B}_2(r) = \bigcup_{i=m+1}^{m+n} W_i([0, T^i(r)]). \tag{3}$$

¹ We refer to (see [32, p. 344])

$T_i(r) = \inf\{t \geq 0 : W_i^i \notin B(0, r)\}$ (W^i is a d -dimensional Brownian motion)

as the exit time from the open ball $B = (0, r) = \{x \in \mathbb{R}^d : q(0, x) < r\}$, where q is the distance in \mathbb{R}^d .

The event that two packets of Brownian paths fail to intersect has a decreasing probability as $r \uparrow \infty$. Using subadditivity, it can be shown that there exists a constant $0 < \xi_d(m, n) < \infty$ such that

$$P\{B_1(r) \cap B_2(r) = \emptyset\} = r^{-\xi_d(m,n)+o(1)} \tag{4}$$

as $r \uparrow \infty$.

The numbers $\xi_d(m, n)$ are called the *intersection exponents* (for more details see [25]).

Then, we consider a number of Brownian motion paths started at different points. As known the intersection among the paths depends on the dimension.

From a mathematical point of view our aim can be formulated in term of the following theorem [30, p. 172].

Theorem 1 (Dvoretzky, Erdős, Kakutani, Taylor). *Suppose $d \geq 2$ and*

$$\{B_1(t) : t \geq 0\}, \dots, \{B_p(t) : t \geq 0\}$$

are p independent d -dimensional Brownian motions started in the origin. Let $S_1 = B_1(0, \infty), \dots, S_p = B_p(0, \infty)$ be their ranges. Then, almost surely

$$S_1 \cap \dots \cap S_p = \{0\} \quad \text{if and only if } p(d-2) \geq d$$

and otherwise

$$\dim(S_1 \cap \dots \cap S_p) = d - p(d-2) > 0.$$

3. Astrophysical context

In [14,15], the authors presented a study on the dynamical systems on Cantorian space–time to explain some relevant stochastic and quantum processes, where the space acts as harmonic oscillating support, such as it often happens in Nature. The role of oscillating structures is played by cosmological objects as globular cluster, galaxies, clusters and superclusters of galaxies through their spatial lengths [33,34]. Table 1 recalls the dimensions and masses of the previous systems [19].

In [5,8,16,17], the first author of the present paper considered the compatibility of a Stochastic Self-Similar Universe with the observation and the consequences of the model. Indeed, it was demonstrated that the observed segregated Universe is the result of a fundamental self-similar law, which generalizes the Compton wavelength relation, $R(N) = (h/m_n c)N^\phi$. A typical interaction length can be defined as a quantity, which is proportional to the size of the system which contains the constituents N (nucleons) [20].

In general, the authors evaluate the number of nucleons in a self-gravitating system as

$$N = \frac{M}{m_n},$$

where N is the number of nucleons of mass m_n into self-gravitating system of total mass M . Then, they obtain the relevant results recalled in Table 2. In the second column the number of evaluated nucleons is shown, while we find the expected radius of self-gravitating system in the last column.

Moreover, the relation

$$R(N) = \frac{h}{Mc} N^\alpha = \frac{h}{m_n c} N^\phi \tag{5}$$

can be written in terms of Plankian quantities:

$$R_p(N) = \frac{l_p}{m_p} \sqrt{\frac{\hbar c}{G}} N^{(1+\phi)} \tag{6}$$

Table 1

Classification of astrophysical systems by length and mass, where h is the dimensionless Hubble constant whose value is in the range [0.5, 1]

System type	Length	Mass (M_\odot)
Globular clusters	$R_{GC} \sim 10$ pc	$M_{GC} \sim 10^{6-7}$
Galaxies	$R_G \sim 1-10$ kpc	$M_G \sim 10^{10-12}$
Cluster of galaxies	$R_{CG} \sim 1.5 h^{-1}$ Mpc	$M_{CG} \sim 10^{15} h^{-1}$
Supercluster of galaxies	$R_{SCG} \sim 10-100 h^{-1}$ Mpc	$M_{SCG} \sim 10^{15-17} h^{-1}$

Table 2
Evaluated length for different self-gravitating systems

System type	Number of nucleons	Eval. length
Glob. clusters	$N_G \sim 10^{63-64}$	$R_{GC} \sim 1-10$ pc
Galaxies	$N_G \sim 10^{68}$	$R_G \sim 1-10$ kpc
Cluster of gal.	$N_{CG} \sim 10^{72}$	$R_{CG} \sim 1$ h ⁻¹ Mpc
Superc. of gal.	$N_{SCG} \sim 10^{73}$	$R_{SCG} \sim 10-100$ h ⁻¹ Mpc

and from Eq. (6) we obtain

$$R_p(N) \propto l_p N^{3/2},$$

where we have assumed $\phi = 1/2$.

If we consider the R radius as a fixed quantities, equalizing Eqs. (5) and (6), we get

$$\frac{l_p}{m_p} \sqrt{\frac{\hbar c}{G}} N^{3/2} = \frac{h}{Mc} N^{3/2}$$

and so

$$M = \frac{m_p}{l_p} \sqrt{\frac{Gh}{c^3}}. \quad (7)$$

In other words, the mass M of the structure is written in terms of Plank's length. As reported in [21,5], the following theorems can be obtained.

Theorem 2. *The structures of Universe appear as if they were a classically self-similar random process at all astrophysical scales. The characteristic scale length has a self-similar expression*

$$R(N) = \frac{h}{Mc} N^{1+\phi} = \frac{h}{m_n c} N^\phi,$$

where the mass M is the mass of the structure, m_n is the mass of a nucleon, N is the number of nucleons into the structure and ϕ is the Golden Mean value.

In terms of Plankian quantities the scale length can be recast in

$$R_p(N) = \frac{l_p}{m_p} \sqrt{\frac{\hbar c}{G}} N^{(1+\phi)}.$$

The previous expression reflects the quantum (stochastic) memory of Universe at all scales, which appears as a hierarchy in the clustering properties.

Theorem 3. *The mass and the extension of a body are connected with its quantum properties, through to the relation*

$$E_{E,N}(N) = E_p N^{1+\phi},$$

that links Plank's and Einstein's energies.

4. Application to cosmology: Brownian multifractals structures

Brownian paths have rich fractal structure, as we have seen in previous section. However, the path is usually qualified as a monofractal, in view that the Holder exponent of the path is everywhere 1/2 (the variations of the regularity are only of a logarithmic order of magnitude). Thus, it is a first approximation to use Brownian path as a curve fitting to those data exhibiting the intermittence. In [20], the authors noted that all astrophysical scales have a particular length. For this reason, they obtained the lengths of the self-gravitation system just by using the previous power law. As a macroscopic system, Universe shows a sort of quantum and relativistic memory of its primordial phase. The choice to start with a $\alpha = 1/2$ is suggested by the Statistical Mechanics.

Indeed Eq. (5) is strictly equivalent to

$$R(N) = l N^\alpha, \quad (8)$$

where $l = h/m_n c$. The relation (8) is the well-known Random Walk or Brownian motion.

In a previous article [4], the authors considered a segregated Universe as the result of an aggregation process, in which a test particle in its motion in the Fractal Cantorian $\epsilon^{(\infty)}$ space–time can be captured or not.

They show that $R(N) = (h/m_n c)N^\phi$, the law represents the observed segregated Universe as the result of a fundamental self-similar law, is a Brownian motion with drift:

$$\tilde{B}_N = B_N + \phi^3 N, \tag{9}$$

where $\phi = (\sqrt{5} - 1)/2$.

Let $B(N)$ be a real-valued Brownian motion (or a fractional Brownian motion if one count the long-range dependent), and let $M(N)$ be an increasing process (that is, a process which is pathwise increasing in N) [24]. Assume that B and M are totally independent (quite rough from the viewpoint of practical applications). The application $N \rightarrow B(M(N))$ is named *Brownian motion in multifractal time*. The path of the new process has some multifractal (=intermittent) structure and some dimension spectrum can be computed.

In order to construct a multifractal cosmological’s scenario the ingredients are: a multifractal “time warp”, i.e., an increasing function or process $M(N)$, for which the multifractal formalism is known, and a function or process B with strong monofractal scaling properties such as considered Brownian motion (Eq. (9)). Let us recall the method of *midpoint displacement* which can be used to define simple Brownian motion $B_{1/2}$ iteratively at dyadic points. Indeed, the increments of the Brownian motion in multifractal time become independent Gaussian once the path of $M(N)$ is realized.

In case that M is a subordinator, then the resulting process is a Lévy process. This case is also known in probability as *Brownian (time) substitution*. We recall that a Lévy process is a stochastic process (real-valued or vector-valued) with stationary and independent increments, and that a subordinator is a real-valued Lévy process with increasing paths.

Jaffard in [22] proved that the paths of “most” Lévy processes are multifractals and he also determined their spectrum of Holder exponents.

Since, the Brownian motion is an example of Lévy processes that can be defined as a monofractal (see Section 2), here, we continue that study by considering the intersection of the exponents of the Brownian motion paths to obtain the multifractal model in the context of Cantorian $\epsilon^{(\infty)}$ space–time.

4.1. Multifractal universe

We consider a Boundaryless Fractal Model of Universe in (3 + 1)-dimension (for more detail see “The Origin of Universes” by Nagasawa [31]). Assume that a distribution of points in i -space, fractal set (like a structures S_i of the

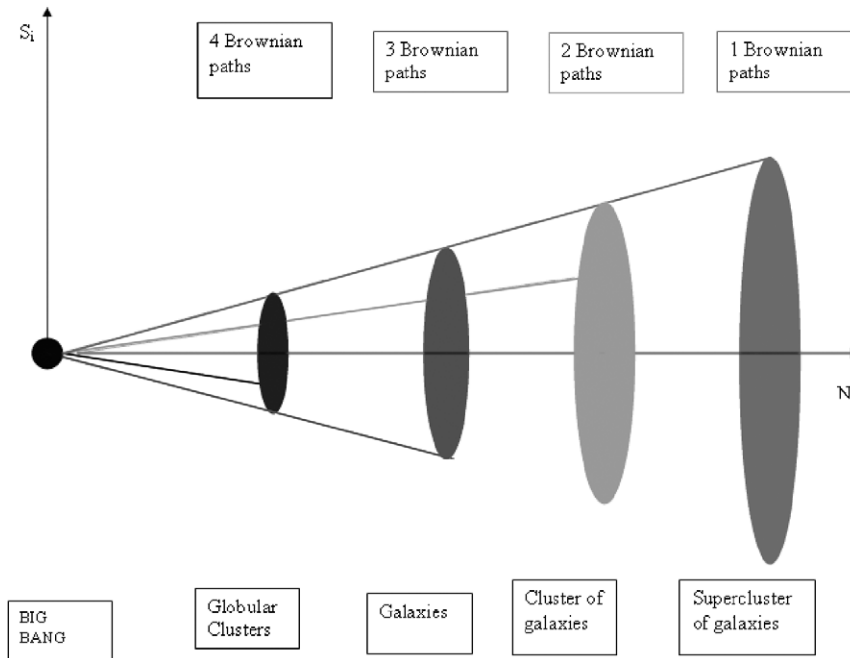


Fig. 1. Model of Universe with Brownian paths.

physical space S) is given from the measure μ : the probability for a point to fall in a set S_i is $\mu(S_i)$. The spatial distribution of points is on a ball of radius $R_i(t)$ and hence, the different structures have a fixed radius $R_i(N)$ and thanks an aggregation process (like Brownian motion) after a fixed time it reaches the mass M_i . Each structure belongs to one different scale on the N -axis (see Fig. 1).

If this distribution is singular one cannot describe it by means of a density and multifractal analysis useful in characterizing the complicated geometrical properties of μ . In our case, we have more Brownian paths, indeed, everyone constructs a specific length scale (like galaxies, globular cluster, etc.). Let us consider a bunch of p independent Brownian motions W_1, \dots, W_p starting uniformly on $\partial S(0, 0)$ in \mathfrak{R}^d (with $d \geq 2$); we call their first exit times N_1, \dots, N_p the time to emerge from a large ball, that is a sort of segregated inflation. Indeed, in our model (as in Fig. 1) we start with four Brownian motions and in different time steps they arrive on the different balls. For this reason we have in the first structure the intersection of four paths, in the second structure the intersection of three paths and so on. In relation to Universe's structure at the end we obtained just one Brownian motion. By classical results of Dvoretzky, Erdős, Kakutani, Taylor (see Theorem 1) the intersection of the paths of these motions is

Table 3
Space–time fractal dimension of astrophysical objects

System type	D
Globular clusters	4.61–4.66
Galaxies (giant)	4.27–4.54
Galaxies (dwarf)	4.18–4.39
Clusters of galaxies	4.20
Superclusters of galaxies	3.94–4.15
Universe	4.13

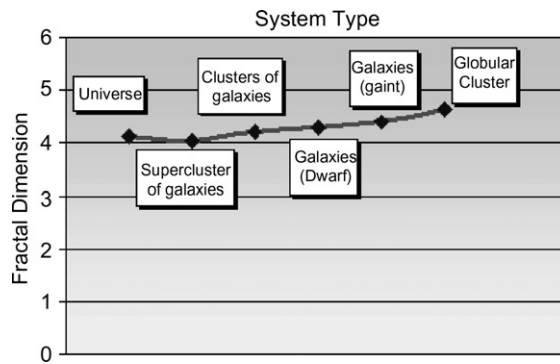


Fig. 2. Trend of space–time fractal dimension of astrophysical objects.

Table 4
Space–time fractal dimension of solar system objects

Solar system objects	Radius (10^6 m)	Mass (kg)	N	D
Sun	6.96×10^2	M_{\odot}	1.1892×10^{57}	7.4546
Mercury	2.439	3.2868×10^{23}	1.9650×10^{50}	8.8741
Venus	6.052	4.8704×10^{24}	2.9112×10^{51}	8.5884
Earth	6.378	5.976×10^{24}	3.5728×10^{51}	8.5761
Mars	3.3935	6.3943×10^{23}	3.8229×10^{50}	8.7454
Jupiter	71.4	1.8997×10^{27}	1.1358×10^{54}	7.8828
Saturn	59.65	5.6870×10^{26}	3.4000×10^{53}	7.8845
Uranus	25.6	8.6652×10^{25}	5.1806×10^{52}	8.1156
Neptune	24.75	1.0279×10^{26}	6.1453×10^{52}	8.1398
Pluto	1.1450	1.7928×10^{22}	1.0718×10^{49}	9.0924
Moon	1.738	7.3505×10^{22}	4.3946×10^{49}	8.9555

$$S_i = \bigcap_{k=1}^p \{x \in \mathfrak{R}^d : x = W_k(N) \text{ for some } N \in [0, N_i]\} \tag{10}$$

with $i = 1, \dots, 4$ and contains different points from the starting point if and only if $p < d/(d - 2)$.

This means that in our fractal model, in $(3 + 1)$ -dimensional space we obtain for different ball-structures:

- Globular clusters $S_1(0, R_{GC}(N))$: four intersections of Brownian paths.
- Galaxies $S_2(0, R_G(N))$: three intersections of Brownian paths.
- Cluster of galaxies $S_3(0, R_{CG}(N))$: two intersections of Brownian paths.
- Supercluster of galaxies $S_4(0, R_{SCG}(N))$: just one Brownian path.

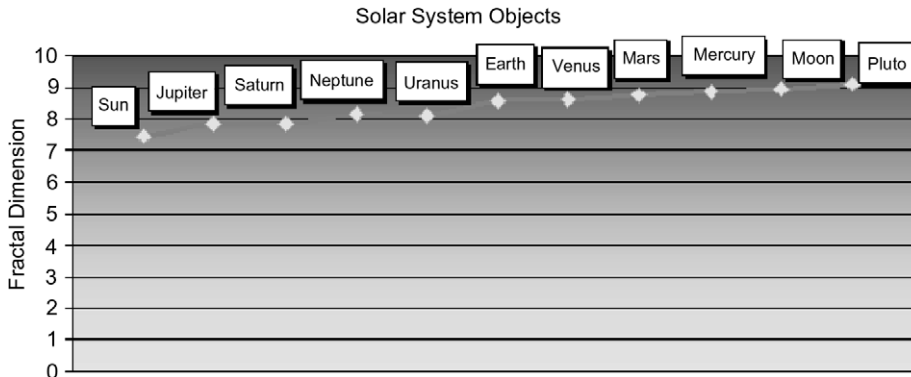


Fig. 3. Graph of fractal dimension of solar system objects.

Table 5
Fractal dimension of atomic elements

Elements	D	Elements	D	Elements	D
H	1	Mn	0.87782	ln	0.85424
He	0.95883	Fe	0.87725	Sn	0.85314
Li	0.94189	Co	0.87559	Sb	0.85233
Be	0.93422	Ni	0.87559	Te	0.85078
B	0.92808	Cu	0.87301	I	0.85103
C	0.92539	Zn	0.8725	Xe	0.85003
N	0.92064	Ga	0.87015	Cs	0.84954
O	0.91651	Ge	0.86881	Ba	0.84858
F	0.91118	As	0.86794	Hf	0.84009
Ne	0.90958	Se	0.86628	Ta	0.83956
Na	0.90524	Br	0.86588	W	0.83902
Mg	0.90390	Kr	0.86432	Re	0.83867
Al	0.90023	Rb	0.86393	Os	0.83797
Si	0.89909	Sr	0.86284	Ir	0.83763
P	0.8959	Y	0.86247	Pt	0.83713
S	0.89491	Zr	0.86175	Au	0.8368
Cl	0.89208	Nb	0.86106	Hg	0.83615
Ar	0.88789	Mo	0.86004	Tl	0.83566
K	0.88868	Tc	0.85971	Pb	0.83518
Ca	0.88789	Ru	0.85841	Bi	0.83487
Sc	0.88417	Rh	0.85778	Po	0.83487
Ti	0.88213	Pd	0.85685	At	0.83472
V	0.88021	Ag	0.85626	Rn	0.8329
Cr	0.87959	Cd	0.85508	Fr	0.83276
				Ra	0.83232

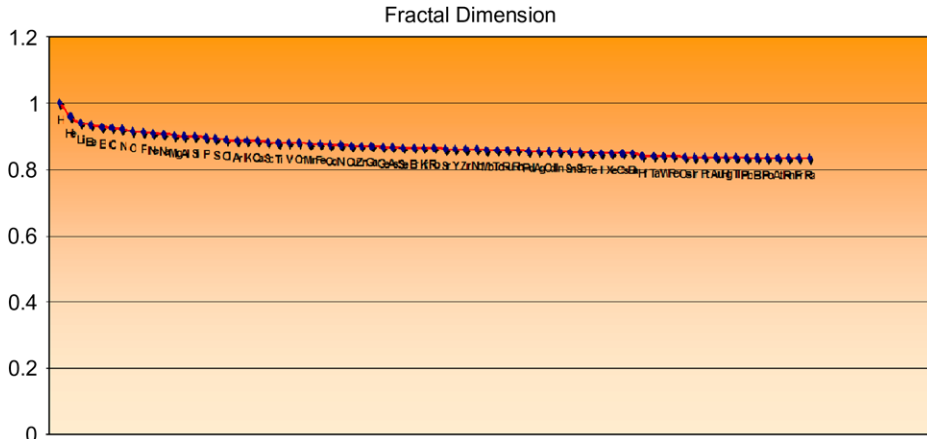


Fig. 4. Graph of space–time fractal dimension of atomic elements.

Table 6
Characteristic parameter time of cosmological structures

System type	Time (s)
Globular cluster	1.0293×10^9
Galaxies	$1.0293 \times 10^{11} - 1.0293 \times 10^{12}$
Cluster of galaxies	$1.5439 \times 10^{14} \text{ h}^{-1}$
Supercluster of galaxies	$1.0293 \times 10^{15} - 1.0293 \times 10^{16} \text{ h}^{-1}$
Universe	6.1756×10^{17}

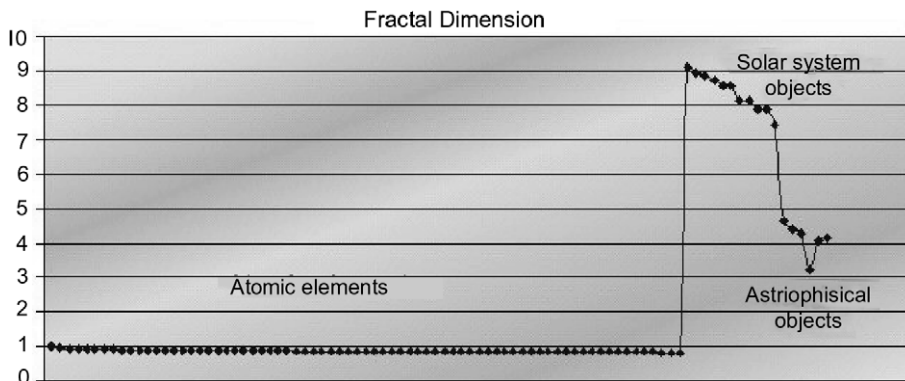


Fig. 5. The space–time fractal dimension model: atomic elements, solar system objects, astrophysical objects.

In order to classify the singularities of μ by strength, we use a Holder exponent and consider the value of the multifractal spectrum (2) which represents the Hausdorff dimension of structures:

$$f_i(a) = \dim \left\{ x \in \mathfrak{R}^d : a = \lim_{R_i(N) \rightarrow 0} \frac{\log \mu(S_i(x, R_i(N)))}{\log R_i(N)} \right\}, \tag{11}$$

where $S_i(x, R_i(N))$ denotes the open ball of radius R_i of the structures centered in x and local dimension a . The structures have the same center $x = 0$ that correspond to the origin of the system (like Big Bang).

Example. For instance, we consider the structure S_i corresponding to a Galaxy with $i = G$ and $R_G \cong 1-10$ kpc. The relation (11) became

Please cite this article in press as: Iovane G et al., Multifractals and El Naschie E -infinity Cantorian space–time, Chaos, Solitons & Fractals (2007), doi:10.1016/j.chaos.2007.07.051

Table 7
Characteristic parameter time for Solar system objects

Solar system objects	Time (s)
Sun	2.3216
Mercury	8.1356×10^{-3}
Venus	2.0187×10^{-2}
Earth	2.1275×10^{-2}
Mars	1.1319×10^{-2}
Jupiter	0.23816
Saturn	0.19897
Uranus	8.5392×10^{-2}
Neptune	8.2557×10^{-2}
Pluto	3.8193×10^{-3}
Moon	5.7973×10^{-3}

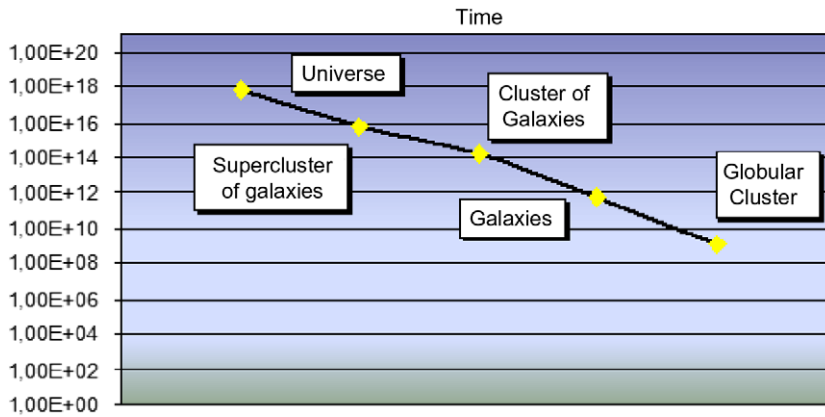


Fig. 6. The characteristic time parameter for cosmological structures.

$$S_G^{[a]} = \left\{ x \in \mathfrak{R}^d : a = \lim_{R_G \rightarrow 0} \frac{\log \mu(S_G(0, R_G))}{\log R_G} \right\}.$$

The center x of the open ball $S(0, R_G)$ is the origin of Universe and it is the same for all structures.

Let us recall that our space–time domain (structure’s domain) is

$$D = \{(x, N); N \geq 0, x \in [-R_i(N), R_i(N)]\} \tag{12}$$

and thank to the result in [20], we can write the dimension (12) as

$$D = \lim_{R_i \rightarrow \infty} \frac{\log(N < R_i)}{\log R_i}, \tag{13}$$

where $N < R_i$ is the number of nucleons inside the radius of the structure R_i .

5. Fractal dimension and time for astrophysical structures

5.1. Fractal dimension

Thanks to (13), we can estimate the fractal dimensions of all astrophysical structure and of Universe too. Hence, the relation (13) represents in this paper our multifractal spectrum.

By recasting (13) in

$$D = \frac{\log(N < R_i)}{\log R_i}, \tag{14}$$

Table 8
Characteristic parameter time for atomic elements

Elements	Time (s)	Elements	Time (s)	Elements	Time (s)
H	5.0165×10^{-24}	Mn	1.9021×10^{-23}	In	2.4319×10^{-23}
He	7.9442×10^{-24}	Fe	1.9125×10^{-23}	Sn	2.4589×10^{-23}
Li	9.5443×10^{-24}	Co	1.9471×10^{-23}	Sb	2.4798×10^{-23}
Be	1.0412×10^{-23}	Ni	1.9445×10^{-23}	Te	2.5189×10^{-23}
B	1.1063×10^{-23}	Cu	1.9966×10^{-23}	I	2.5144×10^{-23}
C	1.1459×10^{-23}	Zn	2.0157×10^{-23}	Xe	2.5431×10^{-23}
N	1.2061×10^{-23}	Ga	2.0593×10^{-23}	Cs	2.5534×10^{-23}
O	1.2608×10^{-23}	Ge	2.0872×10^{-23}	Ba	2.5815×10^{-23}
F	1.3351×10^{-23}	As	2.1093×10^{-23}	Hf	2.8171×10^{-23}
Ne	1.3622×10^{-23}	Se	2.1466×10^{-23}	Ta	2.83×10^{-23}
Na	1.4227×10^{-23}	Br	2.1551×10^{-23}	W	2.8451×10^{-23}
Mg	1.4493×10^{-23}	Kr	2.1895×10^{-23}	Re	2.8572×10^{-23}
Al	1.5007×10^{-23}	Rb	2.2040×10^{-23}	Os	2.8775×10^{-23}
Si	1.5209×10^{-23}	Sr	2.2223×10^{-23}	Ir	2.8876×10^{-23}
P	1.5713×10^{-23}	Y	2.2331×10^{-23}	Pt	2.9019×10^{-23}
S	1.5895×10^{-23}	Zr	2.2523×10^{-23}	Au	2.9112×10^{-23}
Cl	1.6437×10^{-23}	Nb	2.2661×10^{-23}	Hg	2.9289×10^{-23}
Ar	1.7104×10^{-23}	Mo	2.2906×10^{-23}	Tl	2.9472×10^{-23}
K	1.6982×10^{-23}	Tc	2.2990×10^{-23}	Pb	2.9607×10^{-23}
Ca	1.7123×10^{-23}	Ru	2.3306×10^{-23}	Bi	2.9692×10^{-23}
Sc	1.7791×10^{-23}	Rh	2.3447×10^{-23}	Po	2.9693×10^{-23}
Ti	1.8171×10^{-23}	Pd	2.3709×10^{-23}	At	2.974×10^{-23}
V	1.8548×10^{-23}	Ag	2.3818×10^{-23}	Rn	3.0296×10^{-23}
Cr	1.8675×10^{-23}	Cd	2.4147×10^{-23}	Fr	3.0342×10^{-23}
				Ra	3.0478×10^{-23}

we obtain the fractal dimension of different structures. This recast makes sense due to we are summing that for $R > R_i$ the structure of length scale R_i do not take other N and so other matter. Indeed, in the following tables we summarize these results.

Thank to relation (14) and values of Tables 1 and 2 we can calculate the Fractal dimension of astrophysical objects (see Table 3).

In the following graph (Fig. 2) we have ordered the objects for considering their Mass in terms of Solar Mass M_\odot (see Table 1) where

$$M_\odot = 1.98892 \times 10^{30} \text{ kg.}$$

Table 4 summarizes the results with respect to solar system objects.

In the last column in Table 4 we have calculated the Fractal dimension of the Solar system objects.

In the following graph (Fig. 3) we have ordered the objects to considering their Solar Mass.

The previous results suggest a Solar System that lives in a fractal space–time with extra-dimension or in a conventional (3 + 1) space–time but with a presence of dark energy to reduce the extra-dimensions. In Table 5, we calculate space–time Fractal dimensions for atomic elements. In Fig. 4, we show the fractal dimension of 73

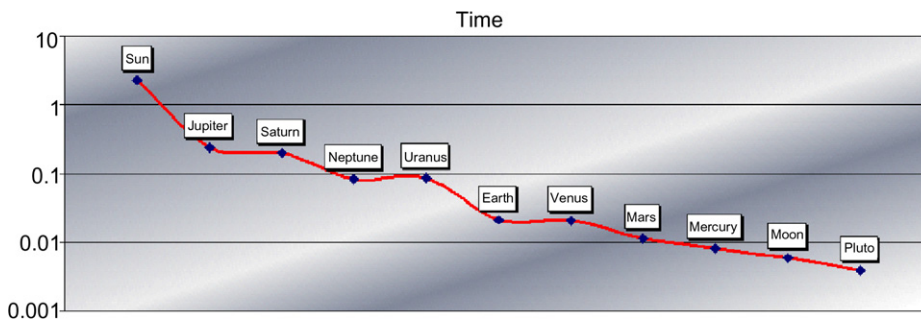


Fig. 7. Characteristic parameter time for solar system objects.

elements of the table because we have not considered the Lanthanoids, Actinoids and the elements from 89 and so on, while Fig. 5 gives us the Fractal dimensions at different scales.

The fact that we obtain a space–time Fractal Dimension with a value that is smaller than 1 suggests that these elements are not stable but tend to create stable chemical links.

5.2. Characteristic parameters of time

In addition, to the Theorems in Section 3, we can evaluate the characteristic parameters of the time of Universe. As we see below it can be written as a function of its components N . Indeed, starting from the relation

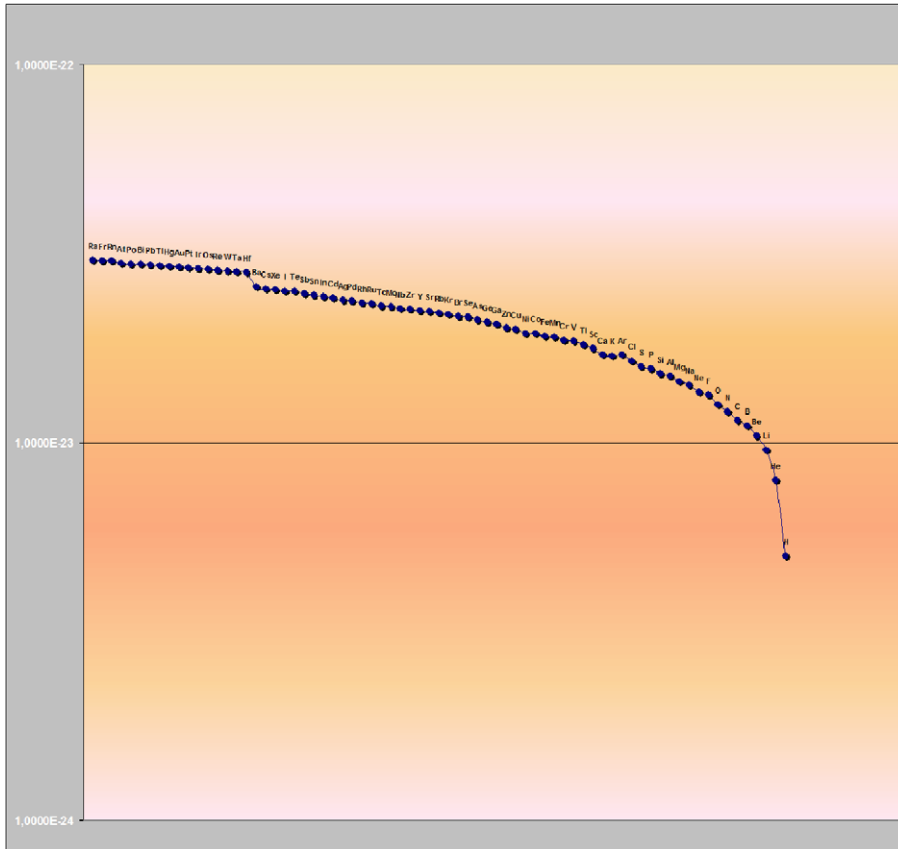


Fig. 8. Characteristic parameter time for atomic elements.

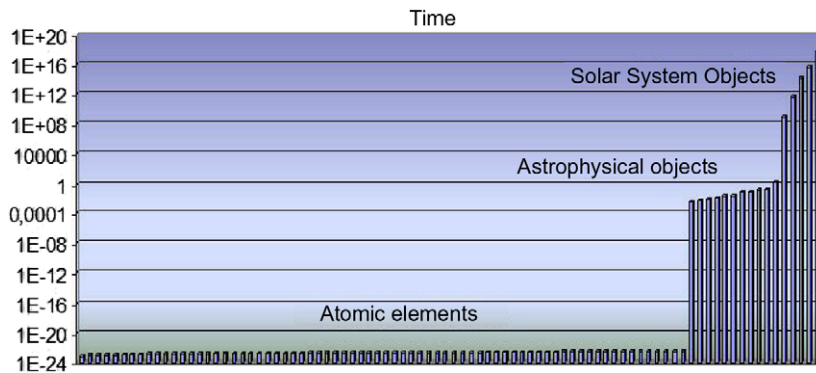


Fig. 9. Characteristic parameter time at all scales.

$$R_U = cT_U, \quad (15)$$

where R_U is the radius of Universe, T_U its time and $c = 2.99792458 \times 10^8 \text{ m s}^{-1}$ by using the relation (7), we easily obtain

$$T = \frac{h}{E_E} N^\phi, \quad (16)$$

where E_E is the Einstein energy for a nucleon, that is $E_E = m_c c^2$.

The relation (16) appears interesting since it connects the characteristic parameters of the time of Universe with the number of its components through quantum and relativistic contents. In Table 6, we calculate the characteristic time parameter for Cosmological structures, where $h = 6.6260755 \times 10^{-34} \text{ J s}$ (see Fig. 5).

Table 7 summarizes the results with respect to the Solar System objects (see Fig. 6).

Table 8 summarizes the results with respect to the periodic table of elements.

What is the meaning of this characteristic time? If we assume T_U as the age of Universe the other times can be seen as a thermalization time, that is the time which different structures take to start the dynamics as we know now. In other words, it is a sort of fluctuation before the structures born or emerge from their quantum or chaotic status (see Figs. 7–9).

6. Conclusions

In this paper, we have considered the link between the scale invariant law, $R(N) = (h/m_n c) N^\phi$, introduced by authors as a Brownian motion, with drift of the form: $\bar{B}_N = B_N + \phi^3 N$, and *Multifractal processes*.

We have used the tools of multifractal in the context of Mohamed El Naschie's $\epsilon^{(\infty)}$ Cantorian space–time applied as to cosmology. In order to prove the multifractal nature of the cosmological's scenario we built a multifractal process. Brownian motion is an example of Lévy process. Thus it is qualified as *monofractal*, because its Hölder exponent is everywhere 1/2. However, in general, most Lévy processes are multifractal. Furthermore, we have considered a Brownian motion in a *multifractal time* and calculated the intersection of the exponent for obtaining a multifractal process starting from a Brownian motion.

In conclusion, we showed some physical consequences with respect to the Fractal Dimension of Cantorian time and we discovered a characteristic parametric time linked to the quantum or chaotic fluctuation preceding the inception of the structures.

References

- [1] Huillet T, Jeannet B. Random walk models for multifractals. *J Phys A: Math Gen* 1994;27:6315–34.
- [2] Riedi RH. Introduction to multifractals. <http://www.dsp.rice.edu/publications/>.
- [3] Li Y, Dai C. A multifractal formalism in a probability space. *Chaos, Solitons & Fractals* 2006;27:57–73.
- [4] Iovane G, Chinnici M. Stochastic self-similar processes and random walk in nature. *J Interdisciplinary Math* 2006;9(3):475–98.
- [5] Iovane G. Mohamed El Naschie's $\epsilon^{(\infty)}$ Cantorian space–time and its consequences in cosmology. *Chaos, Solitons & Fractals* 2005;25(4):775–9.
- [6] Iovane G. Cantorian spacetime and Hilbert: part I – Foundations. *Chaos, Solitons & Fractals* 2006;28(4):857.
- [7] Iovane G. Cantorian spacetime and Hilbert space: part II – relevant consequences. *Chaos, Solitons & Fractals* 2006;29(1):1–22.
- [8] Iovane G, Varying G. Accelerating universe, and other relevant consequences of a stochastic self-similar and fractal universe. *Chaos, Solitons & Fractals* 2004;20(4):657–67.
- [9] Cook TA. *The curves of life*. London: Constable and Company; 1914. Reprinted by Dover Publications, New York. See also: El Naschie MS. Multidimensional Cantor-like sets ergodic behaviour. *Speculation Sci Technol* 1992;15(2):138–42.
- [10] Vajda S. *Fibonacci and Lucas numbers and the Golden section*. New York: J. Wiley; 1989.
- [11] El Naschie MS. A guide to the mathematics of E -infinity Cantorian space–time theory. *CSRF* 2005;25(5):964–95.
- [12] El Naschie MS. On the unification of the fundamental forces and complex time in the $\epsilon^{(\infty)}$ space. *Chaos, Solitons & Fractals* 2000;11:1149–62.
- [13] Sidharth BJ. *Chaos, Solitons & Fractals* 2000;11(2):155; Sidharth BJ. *Chaos, Solitons & Fractals* 2001;12:795.
- [14] Iovane G, Giordano P, Salerno S. Dynamical systems on El Naschie's $\epsilon^{(\infty)}$ Cantorian space–time. *Chaos, Solitons & Fractals* 2005;24(2):423–41.
- [15] Iovane G, Salerno S. Dynamical systems on Cantorian spacetime and applications. *WSEAS Trans Math* 2005;4(3):184.
- [16] Iovane G. Waveguiding and mirroring effects in stochastic self-similar and Cantorian $\epsilon^{(\infty)}$ universe. *Chaos, Solitons & Fractals* 2005;23(3):691–700.

- [17] Iovane G. Self-similar and oscillating solution of Einstein's equation and other relevant consequences of stochastic self-similar and fractal Universe via El Naschie's $\varepsilon^{(\infty)}$ Cantorian space–time. *Chaos, Solitons & Fractals* 2005;23(2):351–60.
- [18] Riedi RH. Multifractal processes, see internet version to <https://centauri.stat.purdue.edu>.
- [19] Abell GO. *Astrophys J S* 1958;3:211.
- [20] Iovane G, Laserra E, Tortoriello FS. Stochastic self-similar and fractal universe. *Chaos, Solitons & Fractals* 2004;20(3):415.
- [21] Iovane G, Giuliano G, Zappale E. A potential theory for describing dynamical systems on El Naschie's $\varepsilon^{(\infty)}$ Cantorian space–time. *Chaos, Solitons & Fractals* 2006;27(3):588–98.
- [22] Jaffard S. The multifractal nature of Levy processes. *Probab Theory Relat Fields* 1999;114:207–27.
- [23] Jaffard S. Mathematical tools for multifractal signal processing. In: Byrnes JS, editor. *Signal processing for multimedia*. IOS Press; 1999.
- [24] Shieh N-R. Some fractal properties of Brownian paths. *Taiwan J Math* 2000;4(1):45–53. March.
- [25] Klenke A, Morters P. The multifractal spectrum of Brownian intersection local times. *Ann Probab* 2005;33(4):1255–301.
- [26] Lawler GF, Schramm O, Werner W. Values of Brownian intersection exponents, I: half-plane exponents. *Acta Math* 2001;187:237–73.
- [27] Lawler GF, Schramm O, Werner W. Values of Brownian intersection exponents, II: plane exponents. *Acta Math* 2001;187:275–308.
- [28] Lawler GF, Schramm O, Werner W. Values of Brownian intersection exponents, III: two-sided exponents. *Ann Inst Henri Poincaré* 2002;38:109–23.
- [29] Halsey TC, Jensen MN, Kadanoff LP, Procaccia I, Shraiman BI. Fractal measures and their singularities. *Phys Rev A* 1986;33:1141–51.
- [30] Morters P, Peres Y. Brownian motion, Draft version of May 8, 2006.
- [31] Nagasawa M. *Stochastic processes in quantum physics*. Birkhauser Verlag; 2000.
- [32] Karatzas I, Shreve SE. *Brownian motion and stochastic calculus*. 2nd ed. USA: John Wiley and Sons, Inc.; 1959.
- [33] Binney J, Tremaine S. *Galactic dynamics*. Princeton: Princeton University Press; 1987.
- [34] Vorontsov-Vel'yaminov BA. *Extragalactic astronomy*. London: Harwood Academic Pub; 1987.